NANO LETTERS

Letter

pubs.acs.org/NanoLett

Stereoelectronic Effect-Induced Conductance Switching in Aromatic Chain Single-Molecule Junctions

Na Xin,[†] Jinying Wang,[†,⊥] Chuancheng Jia,[†] Zitong Liu,[‡] Xisha Zhang,[‡] Chenmin Yu,[‡] Mingliang Li,[†] Shuopei Wang,[§] Yao Gong,[†] Hantao Sun,[∥] Guanxin Zhang,[‡] Zhirong Liu,[†] Guangyu Zhang,[§] Jianhui Liao,[∥] Deqing Zhang,*[,‡] and Xuefeng Guo*[,†,#]

[†]Beijing National Laboratory for Molecular Sciences, State Key Laboratory for Structural Chemistry of Unstable and Stable Species, College of Chemistry and Molecular Engineering, Peking University, Beijing 100871, China

[‡]Beijing National Laboratory for Molecular Sciences, CAS Key Laboratory of Organic Solids, Institute of Chemistry, Chinese Academy of Sciences, Beijing 100190, China

[§]Institute of Physics, Chinese Academy of Sciences, Beijing 100190, People's Republic of China

[∥]Key Laboratory for the Physics and Chemistry of Nanodevices, Department of Electronics, Peking University, Beijing 100871, China

[⊥]Department of Applied Physics, University of Tokyo, Hongo, Tokyo 113-8656, Japan

[#]Department of Materials Science and Engineering, College of Engineering, Peking University, Beijing 100871, China

Supporting Information

ABSTRACT: Biphenyl, as the elementary unit of organic functional materials, has been widely used in electronic and optoelectronic devices. However, over decades little has been fundamentally understood regarding how the intramolecular conformation of biphenyl dynamically affects its transport properties at the single-molecule level. Here, we establish the stereoelectronic effect of biphenyl on its electrical conductance based on the platform of graphene-molecule single-molecule junctions, where a specifically designed hexaphenyl aromatic chain molecule is covalently sandwiched between nanogapped graphene point contacts to create stable single-molecule junctions. Both theoretical and temperature-dependent experimental results consistently demonstrate that phenyl twisting in the aromatic chain molecule produces different microstates with different degrees of conjugation, thus leading to stochastic switching between high- and low-conductance states. These investigations offer new molecular design insights into building functional single-molecule electrical devices.

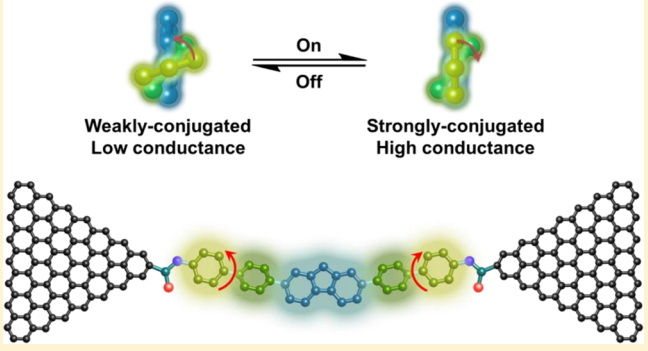

KEYWORDS: *Single molecule junction, switch, biphenyl, stereoelectronic effect*

From its very start, the great potential of molecular electronics, where individual molecules are integrated into electrical circuits, is to meet the increasingly urgent demand for miniaturization of microelectronic devices and their further functionalization.[1,2] Toward this end, over the past several decades, scientists from different disciplinary backgrounds have devoted tremendous effort to develop various molecular junctions with specific functions both theoretically and experimentally, demonstrating a research focus on device functionalization through rational molecular engineering.[3−11] In addition to the future technological vision, the field of molecular electronics is also of fundamental interest, enabling us to probe and understand novel physical and chemical effects at the single-molecule level.[12−15]

Considering both scientific significance and practical application, electrical switches based on molecular junctions have been intensely investigated. In general, specific stimuli-responsive molecules are necessary to realize the switching function in molecular junctions. For instance, photochromic molecules have been used for implementing photoswitching in single-molecule junctions, where photoinduced isomerization occurs under proper light irradiation.[16−21] In another set of remarkable examples using molecules with specific redox centers, the inherent electric field in the junctions can alter the conductance states by changing either their charge states[22] or conformations[23,24] at appropriate bias voltages. In addition to these, regarding mechanically controlled break junction (MCBJ) and scanning tunneling microscope (STM) based molecular devices, external mechanical control of the junction gap can be utilized to alter the conductance state, which might

Received: October 3, 2016
Revised: December 31, 2016
Published: January 10, 2017

DOI: 10.1021/acs.nanolett.6b04139
Nano Lett. 2017, 17, 856−861

result from the corresponding transformation of the molecular orbital level,[25] the change of interface coupling,[26] the stereoelectronic effect,[27,28] or the stretching-induced spin transition.[29] Moreover, the fluctuation at gold−sulfur bonds[30] usually leads to stochastic switching in traditional molecular junctions based on metal electrodes. Toward real-world applications, however, it is still crucial to develop alternative switching mechanisms and operation for constructing reliable molecular switches.

Aromatic chain, especially biphenyl as the elementary unit of organic functional materials, has great potential of extensive applications in organic field-effect transistors (OFET),[31] organic light-emitting diodes (OLED),[32] and solar cells.[33,34] Both experimental and theoretical investigations have suggested that the stereoelectronic effect of the biphenyl-based aromatic structures, namely the variation of twisting angles and corresponding $\pi-\pi$ overlaps between phenyl rings, can significantly influence the structure and photophysical properties of organic functional molecules[35,36] (and thus the performance of the corresponding devices[37]). In particular, theoretical calculations have predicted the temperature-dependent torsion of the biphenyl skeleton[38] and conformation-dependent charge transport through the biphenyl molecule.[39] This prediction strongly suggests the potential use of realizing the switching function with proper design of the biphenyl structures.[40] In the case of terphenyl, there are two different dihedral angles between the outer two benzene rings at each end: one is zero, while the other is almost two times as large as that between the benzene rings in the biphenyl (Figure 1, top).

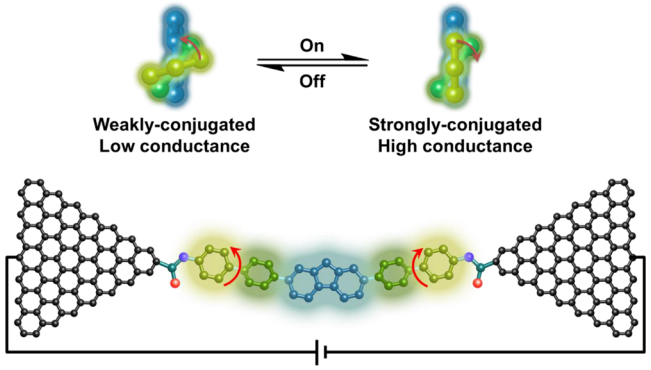

Figure 1. Schematic of conformational transition of terphenyl units between strongly-conjugated and weakly-conjugated states and corresponding hexaphenyl aromatic chain single-molecule junctions.

Intuitively, the $\pi-\pi$ overlap in the former is larger than that in the latter. On the basis of this assumption, we name the former and latter cases as strongly-conjugated and weakly-conjugated, respectively.[41] In the present study, by taking advantage of such stereoelectronic effects of the terphenyl, we aim to explore the temperature-dependent biphenyl torsion and corresponding conductance switching effect in the aromatic chain single-molecule junctions.

Specifically, a hexaphenyl aromatic chain was designed with a symmetrical terphenyl structure, where the medial biphenyl is in a fluorene form to fix the dihedral angle, and amino anchoring groups at two ends. By using nanogapped graphene point contacts fabricated through a dash-line lithographic method described in detail elsewhere,[42] individual aromatic chain molecules were covalently linked to the graphene electrodes with amide bonds to form aromatic chain single-molecule junctions (Figure 1, bottom; Figure S4). Because of the good stability of both graphene electrode materials and covalent amide linkages, the contacts of the fabricated junctions are more robust than metal−sulfur bonds (such as Au−S bonds) in traditional molecular junctions that have the problem with the fluctuation interference,[30] thus ensuring the exploration of the device function from the intrinsic property of the aromatic chain.

To reveal the inherent stereoelectronic effect of the central aromatic chain, conformational characteristics of the hexaphenyl aromatic chain were investigated by using density functional theory (DFT). Through structural optimization and vibrational analysis, three distinct stable conformations (State 1, State 2, and State 3) arising from the variation of the dihedral angles between the phenyl groups were found (Figure 2 and Tables S1−S2). Actually, State 2 can be viewed as a middle state between State 1 and State 3, and the whole conformation changing process is expressed as shown in Figure 2, where T-State 1 and T-State 2 are the transition states between State 1 and State 2 and between State 2 and State 3, respectively. From chemical intuition, a flatter conformation has a higher degree of conjugation. An obvious difference of infrared and Raman spectral features at the wavenumber range of 0−200 cm^{-1} (Figure S6) was observed for the three states. For each state, a vibration mode at ∼80 cm^{-1} corresponds to the twisting of the benzene ring (Figure S10). To clarify the thermodynamic process of conformational changes, the electron energy, enthalpy, and Gibbs free energy of different stable and transition states were calculated, where each value of State 2 was used as the zero-point reference (Figure 2, Table S2). We found that each energy parameter of the three stable states were within ∼1 kJ/mol, while State 3 were relatively higher and State 1 lower. In kinetics, the energy barriers for conformation changes among States 1−3 are determined by T-States 1 and 2, which were predicted to be ∼7 kJ/mol. These calculations set the foundation for the following conductance switching investigation.

On the basis of the investigation of the current−voltage ($I-V$) characteristics of hexaphenyl aromatic chain single-molecule junctions, stochastic switching between two distinct conductance states was indeed observed at 120 K when the bias voltage swept from −0.12 to +0.12 V (Figure 3b). However, within a large bias range this stochastic switching did not occur (Figure S7), excluding the possibility of charge-trap-induced switching.[22] Another important fact we found is that the occurrence of stochastic switching was highly temperature-dependent. The $I-V$ characteristics over the temperature range from 100 to 140 K were shown in Figure 3. Clearly, it can be observed that with increasing the temperature, the switching frequency gradually increased and the current ratio between high/low conductance states gradually decreased. In detail, at 100 K, the device only displayed the typical $I-V$ curves, which correspond to a high conductance state. When the temperature rose to 120 K, stochastic switching between two conductance states started to occur. The switching frequency tends to increase with temperature. Till 140 K, the device nearly stayed in the low conductance state. To gain more information on stochastic switching, the mean dwell times of the high and low conductance states at 120 and 130 K were further extracted out. At 120 K, the mean dwell times of the high and low conductance states were ∼11.4 and ∼5.3 s, respectively. In contrast, at 130 K, the mean time of the device performing the low conductivity remained similar (∼5.1 s) while the high-

DOI: 10.1021/acs.nanolett.6b04139
Nano Lett. 2017, 17, 856−861

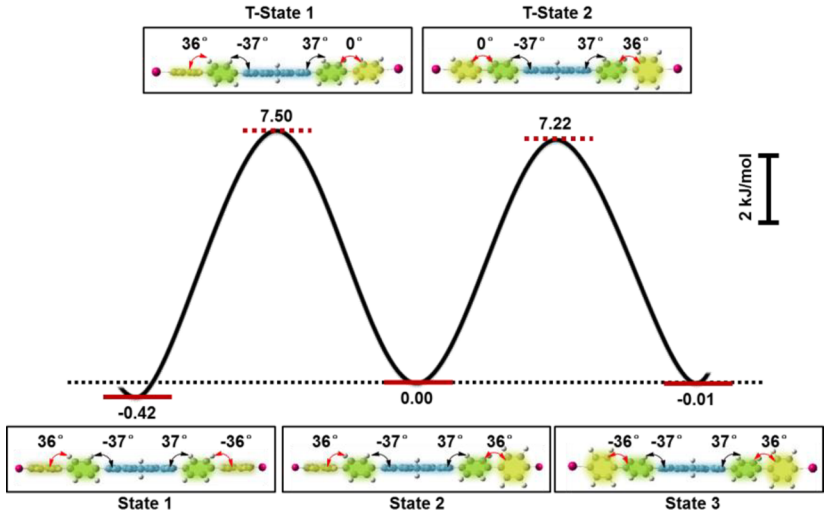

Figure 2. Electron energy diagram of three stable conformations (State 1, State 2, and State 3) and corresponding transition states (T-State 1 and T-State 2) for the hexaphenyl molecule. The configurations for each conformation and transition state are given out with partial dihedral angles marked out. The ended red parts represent the amide linkage (CONH).

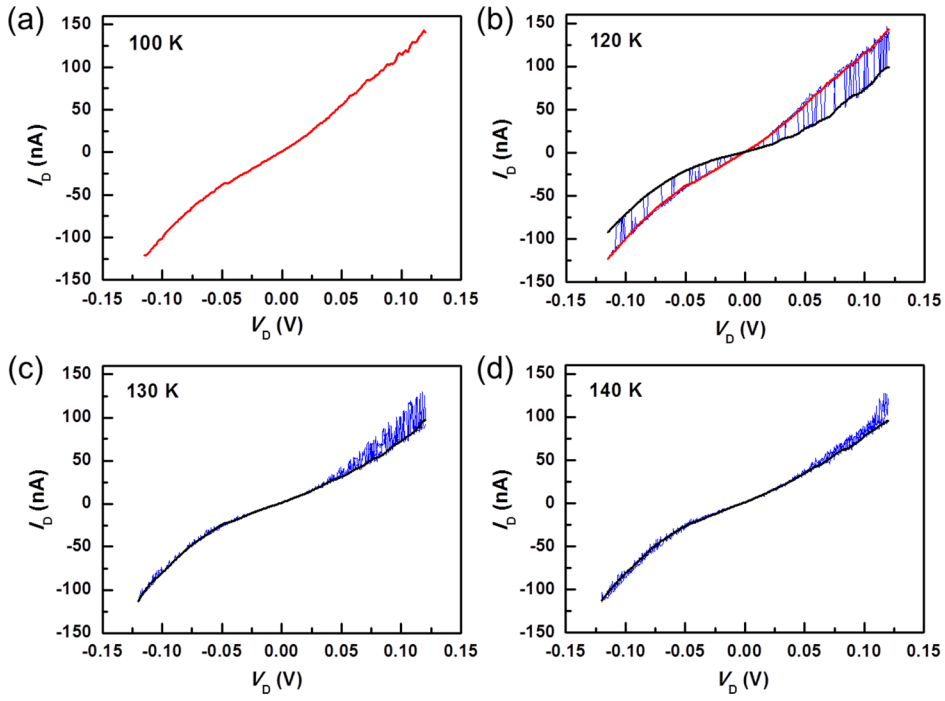

Figure 3. *I*–*V* characteristics for a hexaphenyl aromatic chain single-molecule junction at different temperatures. (a) *I*–*V* curves at 100 K, which show the high conductivity. (b) *I*–*V* curves at 120 K, where the stochastic switching starts to occur. The black and red curves are visual aids for the low and high conductance states. (c) *I*–*V* curves at 130 K showing stochastic switching with higher frequency. (d) *I*–*V* curves at 140 K, where the junction prefers the low conductance state. All *I*–*V* curves are recorded on a single device for at least three times.

conductance lifetime decreased to ∼2.6 s, thus demonstrating that the switching frequency of the devices increased with temperature. Note that stochastic switching at positive biases is stronger than that at negative biases. This asymmetric switching might be due to the asymmetry in the two sides of graphene contacts[43] or other unknown reasons.

We found that the temperature threshold for the conductance switching of molecular junctions was ∼120 K as shown in Figure 3. This implies that above the effective temperature threshold there is enough thermal energy to induce phenyl rotation in the molecule, which ultimately decreases the conjugation and the conductance of the corresponding junction. Although the energy barriers between transition states and stable states of the molecule (∼7 kJ/mol) is higher than the thermal activation energy at 120 K temperature (k_BT, ∼1 kJ/mol), there is a small propability for molecular rotation, which increases greatly with temperature.[44]

As the π–π overlap in State 1 is larger than that in both State 2 and State 3, we hypothesize that the high conductance state corresponds to State 1 of the aromatic chain while the low conductance state corresponds to State 2 and/or State 3. To support this prediction, the transport properties of single-molecule junctions were calculated within the framework of

DOI: 10.1021/acs.nanolett.6b04139
Nano Lett. 2017, 17, 856–861

DFT in combination with a nonequilibrium Green's function method.[45] Specifically, single-molecule junctions with three different configurations were constructed according to State 1, State 2, and State 3 of the aromatic chain (Figure 4 with

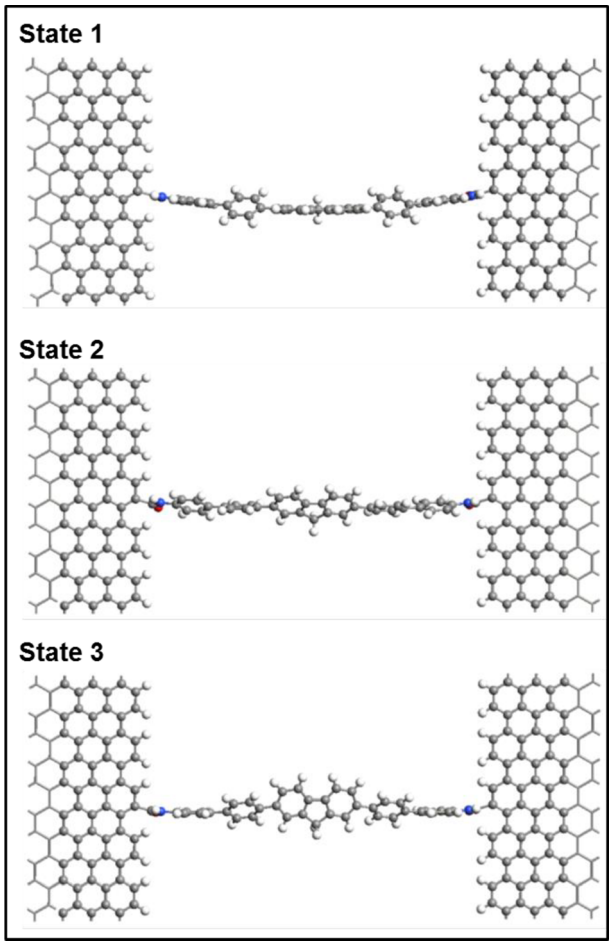

Figure 4. Three different configurations of hexaphenyl aromatic chain single-molecule junctions constructed according to State 1, State 2, and State 3.

armchair-edged graphene electrodes and Figure S14a with zigzag-edged graphene electrodes). From transmission spectra of different junctions at the zero-bias voltage (Figures 5a, S13a, and S14b), it can be observed that only perturbed highest occupied molecular orbital (p-HOMO) transmission peaks are close to the Fermi level, which means that hole transport based on p-HOMO dominates at low bias voltages. Importantly, the transmission coefficient at the Fermi level for State 1 under the zero bias voltage was also much larger than those for State 2 and State 3 (Figures 5a, S13a, and S14b), again leading to the higher conductance for State 1. In addition to these, the $I-V$ curves of the three different molecular junctions were also calculated. From the calculated $I-V$ curves as shown in Figures 5b, S13b, and S14c, it can be observed that the hexaphenyl aromatic chain in State 1 is more conductive than those in State 2 and State 3. Therefore, the above-observed stochastic conductance switching should be attributed to the conformational changes of the aromatic chain, which originates from the torsion of terminal biphenyls at both sides. When the molecule is in State 1, the device shows the high conductance and when it transfers to State 2 or State 3, the conductance switches to the low state accordingly (Figure 5d).

To deeply understand the temperature-dependent switching behavior of molecular junctions, the thermodynamic and kinetic processes of molecular switching were thoroughly discussed. The switching between different conformations consists of four elementary reactions, that is, transformation from State 1 to State 2 and that from State 2 to State 3, and their inverse reactions. The thermodynamic equilibrium constant K_{ij} and reaction rate constant k_{ij} for the reaction from State i to State j can be expressed as $K_{ij} = e^{-\Delta G_{ij}/k_B T}$ and $k_{ij} \propto e^{-E_a^{ij}/k_B T}$, respectively, where ΔG is the free energy change, E_a is the activation energy (free energy difference between the stable state and the transition state), and T is the temperature. At a low temperature (50 K < $T \leq$ 100 K), the molecule remains in a low-enthalpy−energy state (State 1), because k_{12} is too low to promote the conformation switching (although the positive ΔG_{12} is favorable to the transition from State 1 to State 2). When the temperature reaches 120 K, the thermal energy (~1 kJ/mol) is large enough for each reaction (G_{21} = 0.41 kJ/mol, and G_{23} = 1.04 kJ/mol) (Table S2). In the aspect of kinetics, E_a and $k_B T$ start to be at the same order of magnitude in energy, so both the reaction rate constants of the switching from State 2 to State 1 and from State 2 to State 3 begin to jump (Figure 5c). Correspondingly, the conformation changes among States 1, 2, and 3 are observed as demonstrated by conductance switching in $I-V$ plots, and the low conductance state is attributed to State 2 and/or State 3. As the temperature keeps increasing ($T \geq$ 140 K), the $k_B T$ gradually surpasses the absolute value of each ΔG, and the conformational switching becomes so fast that the system reaches its equilibrium quickly. Neither dominating state nor switching process can be experimentally observed at high temperature, and we can only obtain the statistical average results of all three states with averaged conductance.

To support the mechanism discussed above, we also designed and synthesized a control molecule based on a terphenyl structure, in which the neighboring phenyl groups are locked in a fluorene form (Compound 2 in Scheme S2). As demonstrated by theoretical calculations (Figure S15), the three phenyl groups are fixed in a planar conformation. Therefore, on the basis of the investigation of the current−voltage ($I-V$) characteristics of this control terphenyl single-molecular junctions under the same measurement condition, we did observe only one conductance state (Figure S16). This is consistent with the explanation of stereoelectronic effect-induced conductance switching observed in hexaphenyl aromatic chain single-molecule junctions.

In conclusion, we presented here a reliable approach to reveal and understand the stereoelectronic effect on molecular conductivity in a specifically designed hexaphenyl aromatic chain molecule. When the aromatic chain molecule was covalently linked to graphene electrodes to form robust single-molecule junctions, we demonstrated a temperature-dependent stochastic conductance switching originating from thermally-induced random twisting of the phenyl group, which led to strongly conjugated (high conductance) and weakly-conjugated (low conductance) states, as demonstrated both experimentally and theoretically. Such stereoelectronic effect-induced conductance switching investigations provide a fresh perspective for constructing future practical functional single-molecule devices. In addition, these results will also help to

DOI: 10.1021/acs.nanolett.6b04139
Nano Lett. 2017, 17, 856−861

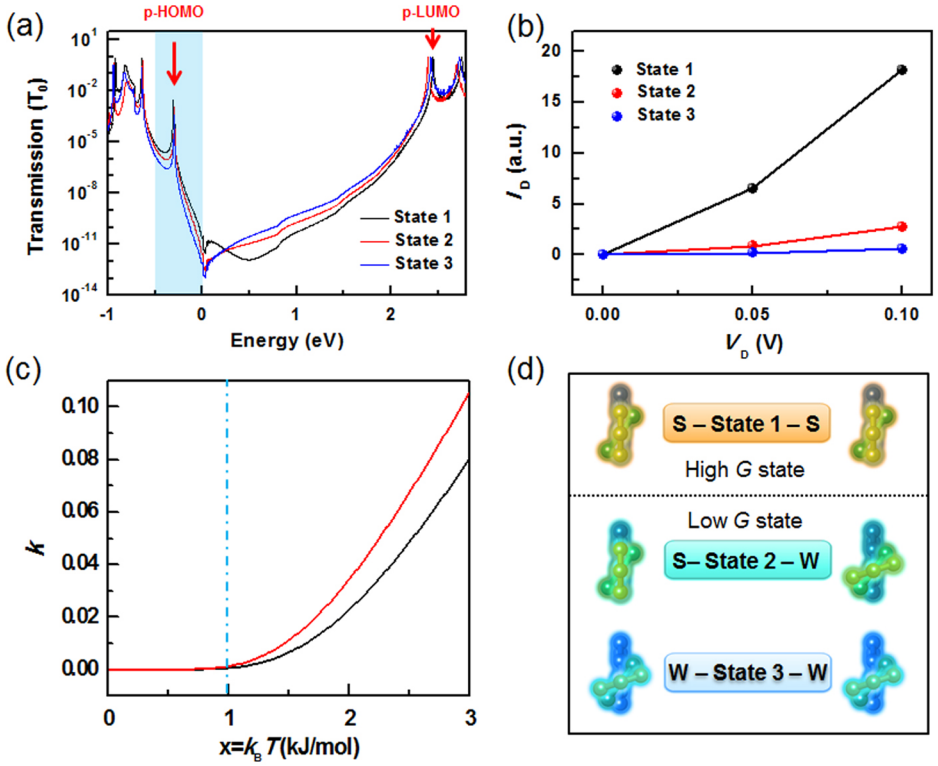

Figure 5. (a) Transmission spectra of hexaphenyl aromatic chain single-molecule junctions under three different configurations (State 1, State 2, and State 3) at a zero-bias voltage. The *k*-point samplings are 99. (b) Calculated *I*−*V* curves for the junctions under different configurations. (c) Plots of the reaction rate constant *k* as a function of temperature *T* for transformation from State 2 to State 1 (red) and that from State 2 to State 3 (black), which clearly shows that when the temperature reaches 120 K (~1 kJ/mol), the reaction rate constant of the switching between different conformations begins to jump. (d) Schematic of the conjugation degree of the aromatic chain molecule at different conformation states, where S represents strongly-conjugated and W represents weakly-conjugated.

design biphenyl-based high-performance organic functional materials for electronic and optoelectronic applications.

■ ASSOCIATED CONTENT

Supporting Information

The Supporting Information is available free of charge on the ACS Publications website at DOI: 10.1021/acs.nanolett.6b04139.

Details of molecular synthesis, device fabrication and characterization, theoretical calculation, and supporting Figures (S1−S16) and Tables (S1−S3) (PDF)

■ AUTHOR INFORMATION

Corresponding Authors

*E-mail: guoxf@pku.edu.cn (X.G.).
*E-mail: dqzhang@iccas.ac.cn (D.Z.).

ORCID

Chuancheng Jia: 0000-0002-1513-8497
Deqing Zhang: 0000-0002-5709-6088
Xuefeng Guo: 0000-0001-5723-8528

Author Contributions

N.X., J.W., C.J., and Z.L. contributed equally to this work.

Funding

This work was supported by the National Natural Science Funds of China (21225311, 91333102, 21373014, and 11222431) and the 973 Project (2012CB921404).

Notes

The authors declare no competing financial interest.

■ REFERENCES

(1) Ratner, M. *Nat. Nanotechnol.* **2013**, *8*, 378−381.
(2) Lörtscher, E. *Nat. Nanotechnol.* **2013**, *8*, 381−384.
(3) Aradhya, S. V.; Venkataraman, L. *Nat. Nanotechnol.* **2013**, *8*, 399−410.
(4) Jia, C.; Guo, X. *Chem. Soc. Rev.* **2013**, *42*, 5642−5660.
(5) Sun, L.; Diaz-Fernandez, Y. A.; Gschneidtner, T. A.; Westerlund, F.; Lara-Avila, S.; Moth-Poulsen, K. *Chem. Soc. Rev.* **2014**, *43*, 7378−7411.
(6) Perrin, M. L.; Burzuri, E.; van der Zant, H. S. J. *Chem. Soc. Rev.* **2015**, *44*, 902−919.
(7) Zhang, J. L.; Zhong, J. Q.; Lin, J. D.; Hu, W. P.; Wu, K.; Xu, G. Q.; Wee, A. T.; Chen, W. *Chem. Soc. Rev.* **2015**, *44*, 2998−3022.
(8) Jia, C.; Ma, B.; Xin, N.; Guo, X. *Acc. Chem. Res.* **2015**, *48*, 2565−2575.
(9) Metzger, R. M. *Chem. Rev.* **2015**, *115*, 5056−5115.
(10) Xiang, D.; Wang, X.; Jia, C.; Lee, T.; Guo, X. *Chem. Rev.* **2016**, *116*, 4318−4440.
(11) Xiang, D.; Jeong, H.; Lee, T.; Mayer, D. *Adv. Mater.* **2013**, *25*, 4845−4867.
(12) Park, J.; Pasupathy, A. N.; Goldsmith, J. I.; Chang, C.; Yaish, Y.; Petta, J. R.; Rinkoski, M.; Sethna, J. P.; Abruna, H. D.; McEuen, P. L.; Ralph, D. C. *Nature* **2002**, *417*, 722−725.
(13) Guedon, C. M.; Valkenier, H.; Markussen, T.; Thygesen, K. S.; Hummelen, J. C.; van der Molen, S. J. *Nat. Nanotechnol.* **2012**, *7*, 305−309.
(14) Perrin, M. L.; Verzijl, C. J. O.; Martin, C. A.; Shaikh, A. J.; Eelkema, R.; van Esch, J. H.; van Ruitenbeek, J. M.; Thijssen, J. M.; van der Zant, H. S. J.; Dulic, D. *Nat. Nanotechnol.* **2013**, *8*, 282−287.
(15) Guo, C.; Wang, K.; Zerah-Harush, E.; Hamill, J.; Wang, B.; Dubi, Y.; Xu, B. *Nat. Chem.* **2016**, *8*, 484−490.

DOI: 10.1021/acs.nanolett.6b04139
Nano Lett. 2017, 17, 856−861

(16) Cao, Y.; Dong, S.; Liu, S.; Liu, Z.; Guo, X. *Angew. Chem., Int. Ed.* **2013**, *52*, 3906−3910.
(17) Jia, C.; Wang, J.; Yao, C.; Cao, Y.; Zhong, Y.; Liu, Z.; Guo, X. *Angew. Chem., Int. Ed.* **2013**, *52*, 8666−8670.
(18) Jia, C.; Migliore, A.; Xin, N.; Huang, S.; Wang, J.; Yang, Q.; Wang, S.; Chen, H.; Wang, D.; Feng, B.; Liu, Z.; Zhang, G.; Qu, D.; Tian, H.; Ratner, M. A.; Xu, H.; Nitzan, A.; Guo, X. *Science* **2016**, *352*, 1443−1445.
(19) Dulic, D.; van der Molen, S. J.; Kudernac, T.; Jonkman, H. T.; de Jong, J. J.; Bowden, T. N.; van Esch, J.; Feringa, B. L.; van Wees, B. J. *Phys. Rev. Lett.* **2003**, *91*, 207402.
(20) Kim, Y.; Hellmuth, T. J.; Sysoiev, D.; Pauly, F.; Pietsch, T.; Wolf, J.; Erbe, A.; Huhn, T.; Groth, U.; Steiner, U. E.; Scheer, E. *Nano Lett.* **2012**, *12*, 3736−3742.
(21) Whalley, A. C.; Steigerwald, M. L.; Guo, X.; Nuckolls, C. *J. Am. Chem. Soc.* **2007**, *129*, 12590−12591.
(22) Schwarz, F.; Kastlunger, G.; Lissel, F.; Egler-Lucas, C.; Semenov, S. N.; Venkatesan, K.; Berke, H.; Stadler, R.; Lörtscher, E. *Nat. Nanotechnol.* **2016**, *11*, 170−176.
(23) Donhauser, Z. J.; Mantooth, B. A.; Kelly, K. F.; Bumm, L. A.; Monnell, J. D.; Stapleton, J. J.; Price, D. W., Jr; Rawlett, A. M.; Allara, D. L.; Tour, J. M. *Science* **2001**, *292*, 2303−2307.
(24) Blum, A. S.; Kushmerick, J. G.; Long, D. P.; Patterson, C. H.; Yang, J. C.; Henderson, J. C.; Yao, Y. X.; Tour, J. M.; Shashidhar, R.; Ratna, B. R. *Nat. Mater.* **2005**, *4*, 167−172.
(25) Bruot, C.; Hihath, J.; Tao, N. J. *Nat. Nanotechnol.* **2012**, *7*, 35−40.
(26) Quek, S. Y.; Kamenetska, M.; Steigerwald, M. L.; Choi, H. J.; Louie, S. G.; Hybertsen, M. S.; Neaton, J. B.; Venkataraman, L. *Nat. Nanotechnol.* **2009**, *4*, 230−234.
(27) Su, T. A.; Li, H. X.; Steigerwald, M. L.; Venkataraman, L.; Nuckolls, C. *Nat. Chem.* **2015**, *7*, 215−220.
(28) Moresco, F.; Meyer, G.; Rieder, K. H.; Tang, H.; Gourdon, A.; Joachim, C. *Phys. Rev. Lett.* **2001**, *86*, 672−675.
(29) Frisenda, R.; Harzmann, G. D.; Celis Gil, J. A.; Thijssen, J. M.; Mayor, M.; van der Zant, H. S. *Nano Lett.* **2016**, *16*, 4733−4737.
(30) Ramachandran, G. K.; Hopson, T. J.; Rawlett, A. M.; Nagahara, L. A.; Primak, A.; Lindsay, S. M. *Science* **2003**, *300*, 1413−1416.
(31) Noh, Y. Y.; Azumi, R.; Goto, M.; Jung, B. J.; Lim, E.; Shim, H. K.; Yoshida, Y.; Yase, K.; Kim, D. Y. *Chem. Mater.* **2005**, *17*, 3861−3870.
(32) Lim, S. F.; Friend, R. H.; Rees, I. D.; Li, J.; Ma, Y.; Robinson, K.; Holmes, A. B.; Hennebicq, E.; Beljonne, D.; Cacialli, F. *Adv. Funct. Mater.* **2005**, *15*, 981−988.
(33) Li, W.; Furlan, A.; Roelofs, W. S.; Hendriks, K. H.; van Pruissen, G. W.; Wienk, M. M.; Janssen, R. A. *Chem. Commun.* **2014**, *50*, 679−681.
(34) Cai, N.; Zhang, J.; Xu, M.; Zhang, M.; Wang, P. *Adv. Funct. Mater.* **2013**, *23*, 3539−3547.
(35) Beenken, W. J.; Lischka, H. *J. Chem. Phys.* **2005**, *123*, 144311.
(36) Greulich, T. W.; Suzuki, N.; Daniliuc, C. G.; Fukazawa, A.; Yamaguchi, E.; Studer, A.; Yamaguchi, S. *Chem. Commun.* **2016**, *52*, 2374−2377.
(37) Venkataraman, L.; Klare, J. E.; Nuckolls, C.; Hybertsen, M. S.; Steigerwald, M. L. *Nature* **2006**, *442*, 904−907.
(38) Arulmozhiraja, S.; Fujii, T. *J. Chem. Phys.* **2001**, *115*, 10589.
(39) Pauly, F.; Viljas, J. K.; Cuevas, J. C.; Schön, G. *Phys. Rev. B: Condens. Matter Mater. Phys.* **2008**, *77*, 155312.
(40) Dou, K. P.; De Sarkar, A.; Wang, C. L.; Zhang, R. Q. *J. Phys. Chem. C* **2011**, *115*, 13911−13918.
(41) Dubi, Y. *J. Chem. Phys.* **2013**, *138*, 114706.
(42) Cao, Y.; Dong, S. H.; Liu, S.; He, L.; Gan, L.; Yu, X. M.; Steigerwald, M. L.; Wu, X. S.; Liu, Z. F.; Guo, X. F. *Angew. Chem., Int. Ed.* **2012**, *51*, 12228−12232.
(43) Fu, X. X.; Zhang, R. Q.; Zhang, G. P.; Li, Z. L. *Sci. Rep.* **2014**, *4*, 6357.
(44) Selzer, Y.; Cabassi, M. A.; Mayer, T. S.; Allara, D. L. *Nanotechnology* **2004**, *15*, S483−S488.
(45) Brandbyge, M.; Mozos, J.-L.; Ordejón, P.; Taylor, J.; Stokbro, K. *Phys. Rev. B: Condens. Matter Mater. Phys.* **2002**, *65*, 165401.

DOI: 10.1021/acs.nanolett.6b04139
Nano Lett. 2017, 17, 856−861